Influence of the Amino-Acid Sequence on the Inverse Temperature Transition of Elastin-Like Polymers

Artur Ribeiro, F. Javier Arias, Javier Reguera, Matilde Alonso, and J. Carlos Rodríguez-Cabello*
G.I.R. Bioforge, Universidad de Valladolid, Centro de I+D, and Networking Research Center on Bioengineering, Biomaterials and Nanomedicine, Valladolid, Spain

ABSTRACT This work explores the dependence of the inverse temperature transition of elastin-like polymers (ELPs) on the amino-acid sequence, i.e., the amino-acid arrangement along the macromolecule and the resulting linear distribution of the physical properties (mainly polarity) derived from it. The hypothesis of this work is that, in addition to mean polarity and molecular mass, the given amino-acid sequence, or its equivalent—the way in which polarity is arranged along the molecule—is also relevant for determining the transition temperature and the latent heat of that transition. To test this hypothesis, a set of linear and di- and triblock ELP copolymers were designed and produced as recombinant proteins. The absolute sequence control provided by recombinant technologies allows the effect of the amino-acid arrangement to be isolated while keeping the molecular mass or mean polarity under strict control. The selected block copolymers were made of two different ELPs: one exhibiting temperature and pH responsiveness, and one exhibiting temperature responsiveness only. By changing the arrangement and length of the blocks while keeping other parameters, such as the molecular mass or mean polarity, constant, we were able to show that the sequence plays a key role in the smart behavior of ELPs.

INTRODUCTION

In addition to their extraordinary potential for elucidating structure-activity relationships in natural proteins, elastin-like polymers (ELPs) are a type of protein-based material that exhibits certain properties that also make them highly attractive for many different advanced applications. The use of ELPs in different fields, such as nanotechnology and biomedicine, has received a great deal of interest in the past few years. Their smart behavior (1), self-assembly (1), complex bioactivity (1), high biocompatibility (1), and the obvious possibility of tuning all of these properties in a feasible and convenient manner have opened the way to new engineered polymer designs with potential performance well beyond the reach of any other family of polymers (2). In addition, due to the peptide nature of these polymers, it is possible to produce them as recombinant proteins in genetically modified organisms (3). In the last few years, the use of recombinant technologies has boosted the level of functionality obtained in these materials and consequently has extended the limits of the range of their potential uses. Biosynthesis allows the production of strictly monodisperse polymers with absolute sequence control and with no possibility of randomness in the comonomer distribution (1). These latter characteristics are highly significant for the applicability of block copolymers as self-assembled systems in nanotechnological applications (4).

The most widely studied ELP is poly(VPGVG), or its recombinant equivalent $(VPGVG)_n$, which is considered a model for ELPs (5). Poly(VPGVG) exhibits a reversible phase transition in response to changes in temperature (5); in other words, it shows an acute thermoresponsive behavior in a process known as inverse temperature transition (ITT). The ITT has frequently been identified with the lower critical solution temperature (LCST) behavior of other smart polymers. However, some phenomenological differences between both transitions make them not completely equivalent. In aqueous solution, below a certain transition temperature, T_t, the free polymer chains remain disordered in the form of random coils (6) that are fully hydrated, mainly by hydrophobic hydration. This hydration is characterized by ordered clathrate-like water structures surrounding the apolar moieties of the polymer (7–10). Above T_t, however, the chain folds hydrophobically and assembles to form a phase-separated state with 63% water and 37% polymer by weight (11), in which, according to Urry's model, the polymer chains adopt a dynamic, regular, nonrandom structure, called a β-spiral, that involves type II β-turns as the main secondary structural feature and is stabilized by intraspiral interturn and interspiral hydrophobic contacts (6). In its folded and associated state, the chain loses essentially all of the ordered water structures resulting from hydrophobic hydration (8). During the initial stages of polymer dehydration, hydrophobic association of the β-spirals results in their taking on a fibrillar form. This process, according to Urry's model, begins with the formation of filaments composed of three-stranded dynamic polypeptide β-spirals that grow to lengths of several hundred nanometers before settling into a visible phase-separated state (6,11). The ITT process is completely reversible and has an associated latent heat, ΔH_t, that results from a combination of the disruption of the water structures and the folding and stabilization resulting from van der Waals contacts (12).

Submitted January 23, 2009, and accepted for publication March 26, 2009.

*Correspondence: roca@bioforge.uva.es

Editor: Jane Clarke.

0006-3495/09/07/0312/9 $2.00

doi: 10.1016/j.bpj.2009.03.030

The existence of this regular secondary structure—the β-spiral—is a matter of some controversy. Some works, such as those by Daggett's group (13,14), have used molecular-dynamics simulation to show that the β-spiral is not a stable structure. Similarly, Gross et al. (15), using the small polypentapeptide $C(GVGVP)_6$, pointed out that the structure in the folded state could be a β-sheet instead of a β-spiral. However, from the point of view of the work reported herein, the precise structure of the folded state of the ELPs used here is not relevant since our interest is restricted to the thermodynamic parameters associated with the ITT, irrespective of the structural 3D arrangement that the chains may adopt in the two states.

Substitution of the second L-valine in the polypentapeptide $(VPGVG)_n$ by every naturally occurring amino acid residue (except L-proline) occurs with retention of the ITT. This substitution affects the position of T_t in a manner related to the polarity of the guest amino acid. This effect is caused by the different ways in which polar and apolar moieties are hydrated (5). Thus, an increase in the polarity of some species decreases the amount of water involved in hydrophobic hydration, whereas a decrease in the polarity of these amino acids increases the hydrophobic hydration. As generally described by Butler (16), and further adapted for ELPs by Urry (17,18), an increase in the amount of water of hydrophobic hydration decreases the solubility of the polymer. An increase in the polarity therefore decreases the hydrophobic hydration, which causes an increase in T_t and, in addition, a decrease in ΔH_t, as this enthalpy is predominantly related to the disruption of the water structures of hydrophobic hydration.

The use of functional amino acids (amino acids that can show two different polarity states in response to a stimulus) makes it possible to obtain a shift in T_t, ΔT_t, as a consequence of the changes in polarity of the side chain. Therefore, as the system is situated in the temperature window between the two T_t values, it exhibits a stimulus smart behavior under isothermal conditions. With the use of this mechanism, different ELPs have been synthesized to respond to different stimuli, such as pH, light, and redox potential (2). For example, changing one L-valine in one of every five pentapeptides by L-glutamic acid is enough to increase T_t by $>40^\circ C$ when the pH exceeds the pK_a (19).

The ELP obtained by substituting the first glycine by an L-alanine, which results in the polymer poly(VPAVG) or the $(VPAVG)_n$, is a special case because it exhibits very different properties. One of these peculiarities is its distinct mechanical behavior. The matrix that results from their cross-linking is more similar to a plastic than to an elastomer, which is the common mechanical nature of the rest of ELPs, with a Young's modulus two orders of magnitude higher than that for cross-linked $(VPGVG)_n$ (20). It also has a different kinetic behavior during its transition (21).

Since the emergence of this new class of materials, the two main thermodynamic characteristics of the ITT (i.e., T_t and the associated latent heat ΔH), and their differences among the different ELPs, have been considered to be an exclusive consequence of the mean polarity of the chain (5) and the molecular mass as intrinsic parameters. Thus, as demonstrated by Meyer and Chilkoti (22), the effect of the molecular mass on T_t decreases as the molecular mass increases. This dependence is not linear, however, and above a certain molecular mass it is almost negligible (19,22), although it is a very important effect at low molecular masss.

The influence of mean polarity and molecular mass as intrinsic factors affecting the ITT is well supported. Indeed, their role is so well established that no other intrinsic parameters have been explicitly considered as playing a potential role. However, all of the experimental data supporting these facts were obtained mainly with homopolymers or regular copolymers with simple molecular architectures. This same simple concept is currently applied to ELPs with more complex amino-acid sequences, even in cases where the pursued application demands a precise prediction of T_t. This is the case, for example, for polymers developed for drug delivery using local hyperthermia (23–25), where T_t should be in a very narrow range of temperatures just above the body temperature. Significant efforts have been made to develop models and expressions to predict the exact T_t values of ELPs based exclusively on calculating the mean polarity of the polymer by considering the polarity of each amino-acid that forms part of the polymer (23,26), without taking into account the way in which polar and apolar amino acids are arranged along the polymer chain. Other relevant examples of complex ELPs and ELP-derived molecules can be found in the use of ELPs to improve the efficiency and ease of purification of a recombinant protein (27). In this case, the protein of interest is conjugated with an ELP to exploit its ITT in the isolation and purification protocols. Again, a clear prediction of the final T_t of the conjugate is a prerequisite for its successful use.

Amphiphilic block ELP copolymers similar to the ones used in this work were shown in previous studies to be excellent candidates for obtaining self-assembling micelles and nanocarriers (28,29). Although the focus in those studies was placed firmly on the final 3D structures arising after the self-assembly process, the influence of the different blocks, mainly regarding their T_t values, is evident. For example, Sallach et al. (28) showed that the T_t of the lateral block is increased by a middle block. Furthermore, using diblocks of different block sizes, Dreher et al. (29) showed that the transition temperature of the more hydrophobic block is affected by the other block, and that this effect decreases when this hydrophobic block is bigger in size relative to the hydrophilic ones. However, in both cases there is no way to determine from the experimental data whether this influence is simply caused by changes in the mean polarity and molecular mass of the studied polymers, or there is an additional contribution from the way the hydrophobic and hydrophilic amino acids are distributed along the polymer chain.

The hypothesis proposed in this work is that the mean polarity of the ELP is not the only intrinsic factor, in combination with the molecular mass, that affects the T_t and ΔH values

in ELPs. On the contrary, we believe that even in ELPs with the same mean polarity and molecular mass, different values of T_t and ΔH can be observed because the constituent amino acids are arranged in a different fashion, which gives rise to different polarity distributions along the polymer chain.

To study the effect of the amino-acid sequence on the T_t and ΔH values, we synthesized different ELP block copolymers as recombinant proteins. These block copolymers are based on two previously studied ELPs, both of which are well characterized. These two polymers are the different blocks used in this work. The first block is $[(VPGVG)_2\text{-}(VPGEG)\text{-}(VPGVG)_2]_n$, a well known pH-responsive smart polymer, and the other is $[VPAVG]_m$, a thermoresponsive polymer with no pH responsiveness. This kind of block ELP, which is similar to those reported by Wright et al. (30) and Wu et al. (31,32), has shown an interesting behavior in terms of micelle formation. In this work, the set of copolymers produced includes three diblock copolymers with a fixed size of the L-glutamic acid-containing block (E-block) and three different sizes of the block that contains the L-alanine residue (A-block; E50A20, E50A40, and E50A60); three triblock copolymers with a variable size of the A-block flanked on both sides by a fixed E-block (E50A20E50, E50A40E50, and E50A60E50); a diblock copolymer with the same molecular mass and block proportion as the middle triblock copolymer (E100A40); a tetrablock copolymer with the same molecular mass and block proportion as the last diblock and the middle triblock copolymers (E50A20E50A20); and, finally, a diblock copolymer with a Leu-$(Gly)_{10}$-Leu linker between the two blocks (E50-G_L-A40). The code used to name the different blocks pertaining to a particular block copolymer includes a letter (E or A) to identify either an E- or an A-block, respectively, and a number indicating the number of pentamers in the block. The homopolymers A62 and E75 were used as controls. These two homopolymers have a molecular mass in the range of those of the block copolymers studied here and are used to identify the individual behavior of the two blocks in the block copolymers.

In general, the blocks that form part of the different copolymer structures were found to be in the soluble-extended state when cooled below their T_t, and in a collapsed-aggregated state above T_t. In addition, the T_t values are directly affected by the pH only for the E-block, due to the presence of glutamic acid in its composition. The A-block is not directly affected by pH since all of the amino acids present in its composition have no lateral chains that can be directly affected by pH changes. A comparison of the T_t and ΔH values for the different block copolymers allowed us to quantify the dependence of these parameters on the amino-acid sequence.

MATERIALS AND METHODS

Materials

Escherichia coli strain XL1-Blue and *Taq* DNA polymerase were obtained from Stratagene (La Jolla, CA). *E. coli* strain BLR(DE3) and pET-25(+) were obtained from Novagen (Madison,WI). T4 DNA ligase and all restriction enzymes were obtained from Fermentas (Burlington, Ontario, Canada). Synthetic oligonucleotides were purchased from IBA GmbH (Goettingen, Germany).

Synthetic gene construction

Cloning and molecular-biology procedures were performed using standard techniques (33,34), and the sequence of all putative inserts was verified by automated DNA sequencing. Synthetic DNA duplexes encoding the oligopeptide $(VPGVG)_2$-(VPGEG)-$(VPGVG)_2$ and the oligopeptide $(VPAVG)_{20}$ were generated by polymerase chain reaction (PCR) amplification using synthetic oligonucleotides. The gene cloning, concatenation, and colony screening were performed as described previously (34).

Expression and purification

Selected genes were subcloned into a modified pET-25(+) expression vector and transformed into the *E. coli* strain BLR(DE3). Expression conditions and purification protocols were as described previously (34). Production yields for all of the polymers were between 80 and 200 $mg \cdot L^{-1}$ of bacterial culture. The final products were characterized by sodium dodecyl sulfate polyacrylamide gel electrophoresis, matrix-assisted laser desorption/ionization-time of flight mass spectrometry, and amino-acid analysis. All of the analyses confirmed the correctness of the biosynthetic process in terms of sequence and molecular mass (Table 1).

Differential scanning calorimetry

Experiments were performed on a Mettler Toledo 822e with liquid-nitrogen cooler. Both temperature and enthalpy were calibrated with a standard sample of indium. The solutions for the differential scanning calorimetry

TABLE 1 Amino-acid sequence of the elastin-like block copolymers investigated (abbreviation indicates the kind of block and the number of pentapeptides in each block)

	Sequence	Molecular mass/kDa	Abbreviation
i	$(VPAVG)_{62}$	26.3	A62
ii	$[(VPGVG)_2\ (VPGEG)\ (VPGVG)_2]_{15}$	31.9	E75
iii	$[(VPGVG)_2\ (VPGEG)\ (VPGVG)_2]_{10}$-$(VPAVG)_{20}$	30.5	E50A20
iv	$[(VPGVG)_2\ (VPGEG)\ (VPGVG)_2]_{10}$-$(VPAVG)_{40}$	38.5	E50A40
v	$[(VPGVG)_2\ (VPGEG)\ (VPGVG)_2]_{10}$-$(VPAVG)_{60}$	47.0	E50A60
vi	$[(VPGVG)_2\ (VPGEG)\ (VPGVG)_2]_{10}$-$(VPAVG)_{20}$-$[(VPGVG)_2\ (VPGEG)\ (VPGVG)_2]_{10}$	51.9	E50A20E50
vii	$[(VPGVG)_2\ (VPGEG)\ (VPGVG)_2]_{10}$-$(VPAVG)_{40}$- $[(VPGVG)_2\ (VPGEG)\ (VPGVG)_2]_{10}$	59.5	E50A40E50
viii	$[(VPGVG)_2\ (VPGEG)\ (VPGVG)_2]_{10}$-$(VPAVG)_{60}$- $[(VPGVG)_2\ (VPGEG)\ (VPGVG)_2]_{10}$	67.9	E50A60E50
ix	$[(VPGVG)_2\ (VPGEG)\ (VPGVG)_2]_{20}$-$(VPAVG)_{40}$	59.5	E100A40
x	$[(VPGVG)_2\ (VPGEG)\ (VPGVG)_2]_{10}$-$LG_{10}L$ -$(VPAVG)_{60}$	47.8	E50-G_L-A60
xi	$[[(VPGVG)_2\ (VPGEG)\ (VPGVG)_2]_{10}$-$(VPAVG)_{20}]$ - $[[(VPGVG)_2\ (VPGEG)\ (VPGVG)_2]_{10}$-$(VPAVG)_{20}]$	59.5	E50A20E50A20

(DSC) experiments were prepared at 50 mg·mL^{-1} and the pH was adjusted by adding small amounts of HCl or NaOH. The use of buffers was avoided to minimize the effect of salts on the ITT. For analysis, 25 μL of the solution were placed inside a standard 40-μL aluminum pan and sealed hermetically. The same volume of water was placed in the reference pan. The heating program of a typical DSC experiment includes an initial isothermal stage (5 min at 5°C for stabilization of the temperature and the state of the polymers), followed by heating at 5°C·min^{-1} from 5°C to 80°C. For the sake of clarity, however, the plots of these results were restricted to the range of 5–65°C, since no further changes were observed in any of the thermograms obtained above the latter temperature.

RESULTS AND DISCUSSION

Fig. 1 *A* shows the individual DSC heating runs for the mixture of two homopolymers $[(VPGVG)_2\text{-}(VPGEG)\text{-}(VPGVG)_2]_{15}$ (E75) and $(VPAVG)_{62}$ (A62) (50% w/w). At acid pH (pH 2.5), the endotherms associated with the corresponding ITTs are evident for both polymers. By comparison with the individual homopolymer thermograms (result not shown), we assume that the first endotherm that takes place corresponds to the transition of E75, and the second one to A62. Of interest, a comparison of the peak temperatures for the cosolution with the results found for the individual homopolymers indicates that even though the ITT is sometimes described as a cooperative phenomenon, the two transitions take place independently and without a significant mutual interchain interaction between the two species. In effect, the peak temperature found for E75 in the cosolution (30.0°C) is only slightly higher than that found for the polymer alone (28.8°C). Such a small difference is likely to be an artifact resulting from the overlapping of that transition with that of A62, which has a higher integral. The second polymer shows a peak temperature of 33.0°C, which matches that found for A62 alone exactly. Similarly, the total enthalpy of the two transitions is 20.4 J · g^{-1}, which corresponds well, within experimental error, with the 50:50 averaged value of the values (9 and 34 J · g^{-1}) found for E75 and A62, respectively. A similar behavior was found in other mixtures with compositions ranging between 0:100 and 100:0, further supporting the absence of mutual interactions in the cosolutions (Fig. 1 *B*). When the DSC experiments were performed at neutral pH (pH 7.0), only the endotherm for the A62 polymer was observed. This pH is well above the pK_a of glutamic acid ($pK_a = 4.5$), which means that this moiety is fully deprotonated. Both the absence of transitions for the E75 polymer and the T_t and ΔH values found for A62 are therefore in agreement with previous findings (19,21).

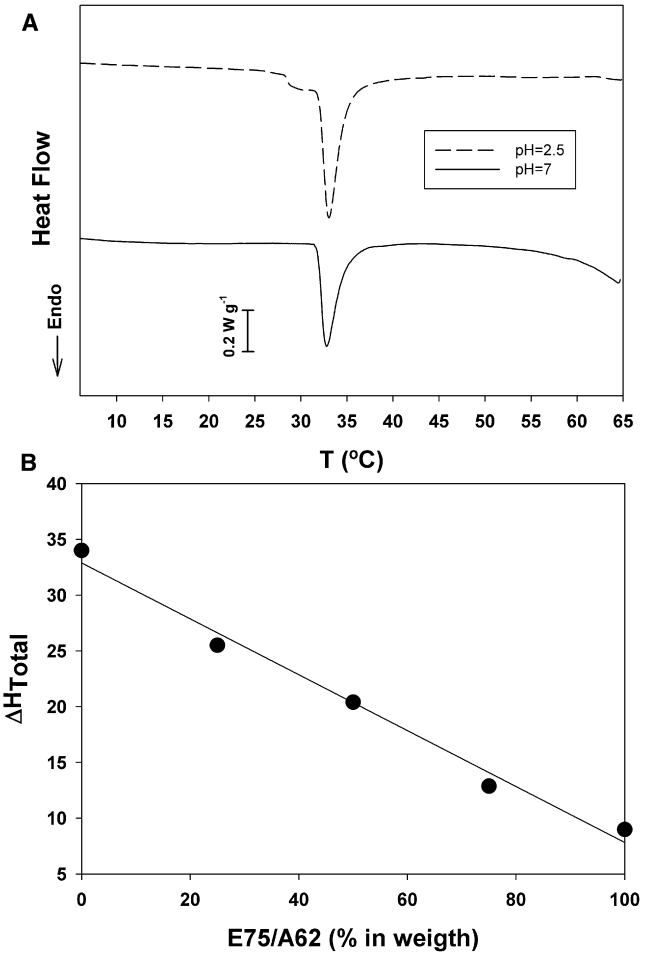

FIGURE 1 (*A*) DSC thermograms in a heating run (5°C·min^{-1}) for an aqueous solution (50 mg·mL^{-1}) of a mixture of $[(VPGVG)_2$ $(VPGEG)$ $(VPGVG)_2]_{15}$ (E75) and $(VPAVG)_{62}$ (A62) (50% w/w) at pH 2.5 and 7.0. (*B*) Latent heat (ΔH_{Total}) vs. E75/A62 (in w/w percentage) for different mixtures of the same polymers at pH 2.5.

In conclusion, despite the fact that the ITT has been considered in the literature as an interchain cooperative phenomenon (18), especially to account for the dependence of T_t and ΔH on the polymer concentration, this interchain cooperativity does not seem to take place between the two kinds of chains in this case, since the different homopolymers behave in an independent fashion when codissolved. As shown below, however, this independent behavior changes completely when these two polymers become blocks in block-copolymer architectures.

Mutual influence in diblock copolymers

DSC thermograms for the diblock copolymer E50A60 are shown at two representative pHs (2.5 and 7.0) in Fig. 2. Fig. 3 shows the quantitative dependence of T_t and ΔH on the pH. At pH 2.5, the two endotherms present in the thermogram overlap in just one peak at 31.9°C, midway between the values found for the cosolution of the two homopolymers (30.0 and 33.0°C). ΔH for this system is 25.4 J · g^{-1}, which is significantly higher than the averaged value of the corresponding homopolymers (ΔH = 20.4 J · g^{-1}). This higher enthalpy indicates a higher degree of hydrophobic hydration.

The mutual influence between the blocks is more evident at pH values above the carboxyl pK_a. The trend of peak temperature and enthalpy of the observed endotherm can be seen in Fig. 3, which clearly shows a shift of the peak temperature close to the pK_a of the carboxyl group present in the E-block. As the pH rise above pK_a, T_t shifts to higher

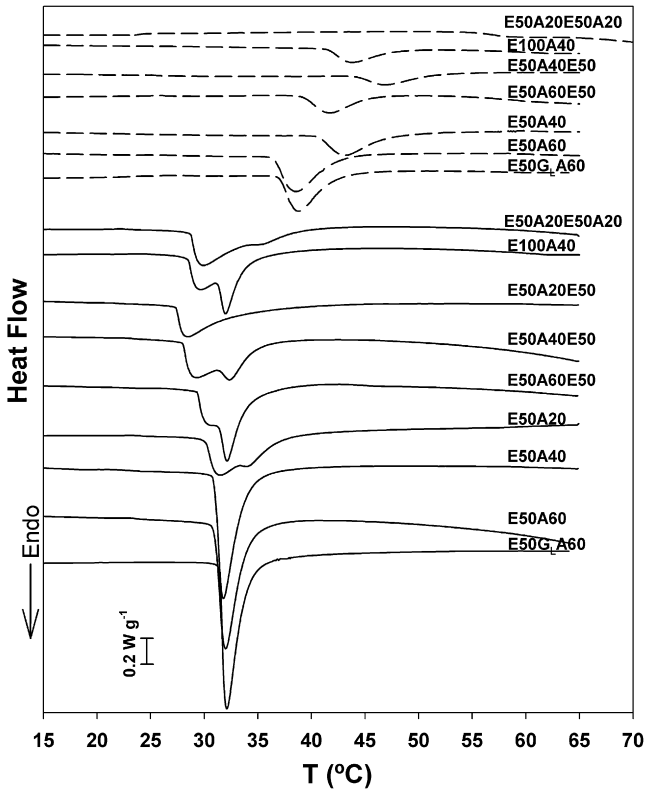

FIGURE 2 DSC thermograms in a heating run ($5^{\circ}C \cdot min^{-1}$) for the different block copolymers at pH 2.5 (*solid*) and pH 7.0 (*dash*).

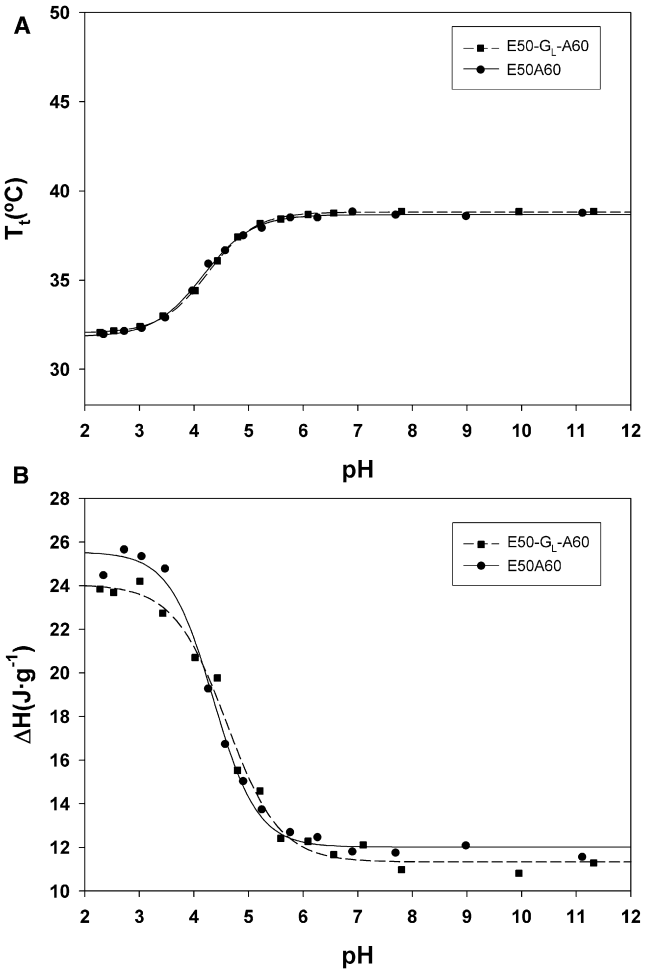

FIGURE 3 Plot of T_t (*A*) and ΔH (*B*) versus pH for the diblock copolymers E50A60 and E50-G_L-A60.

temperatures with a concomitant drop in ΔH. Both curves show a sigmoidal trend versus pH similar to the expected shape for deprotonation (titration) of the carboxyl groups. The substantial decrease in ΔH above the pK_a must therefore be caused by the disappearance of the transition associated with the E-block, as was the case with the cosolution studied previously. However, even though the E-block is now not able to show an ITT at pH values above the pK_a, its presence greatly affects the ITT shown by the A-block. In this diblock, the peak temperature is shifted to 38.6°C, which is 5.6°C higher than that observed in the cosolution, and $\Delta H = 11.8\ J \cdot g^{-1}$, which is clearly lower than the value found in the cosolution ($\Delta H = 16.3\ J \cdot g^{-1}$). Therefore, not surprisingly, the transition of the A-block is clearly affected by the state of the E-block.

In a first approximation, the observed influence can be explained by the standard model for the behavior of ELPs; that is, as the mean polarity of the block copolymer increases, as happens when the E side chains go above the pK_a and become a charged carboxylate, T_t increases and ΔH decreases.

The actual impact of the mean polarity changes on the ITT of the A-block will be studied in more detail later, although an interesting hypothesis should be taken into consideration beforehand. The cosolution experiments show that the interaction between the two blocks cannot be interpreted in terms of interchain interactions; therefore, one evident possibility is an intrachain influence. The most obvious situation is an intrachain cooperativity effect by which the disordering of the E-block propagates its unfolded state to the A-block through the link between the two blocks, thereby causing a shift in the temperature at which the ITT takes place for that A-block. To test this possibility, a new diblock copolymer (E50-G_L-A60) was designed and bioproduced. This block copolymer is similar to E50A60 but contains an additional glycine decamer linker between the two blocks. The glycine decamer does not show any conformational tendency due to the great facility of the glycine bonds to allow almost free rotation along the polymer chain. Therefore, if the disordered or ordered states are able to propagate between the two blocks along the chain in the conventional E50A60 diblock copolymer, this possibility must be significantly reduced by the interposition of the glycine linker between the two blocks. The linker must therefore produce a decoupling effect between the two blocks.

A comparison of the behavior of the two diblock copolymers E50A60 and E50-G_L-A60 can be seen in Fig. 3, which

shows plots of T_t and ΔH as a function of pH for the two polymers. Of interest, the behavior of the two diblocks is almost the same, which means that the presence of the glycine linker has only a minor influence (negligible within the experimental error).

The T_t values for both polymers are very similar, with E50-G_L-A60 showing only a small shift of 0.1°C at pH 2.5 and 0.2°C at pH 7.0 (Fig. 3 *A*). This difference is smaller than the asymptotic standard errors of 0.06 and 0.11°C for the polymers with and without the glycine linker at low pH, and 0.15 and 0.27°C at high pH. The difference for ΔH is again very small (Fig. 3 *B*), being smaller for the copolymer that contains the linker, but again is not significant as it is within the experimental error.

In the case of a successful decoupling of the two blocks at neutral or basic pH, where only the transition associated with the A-block takes place, T_t and ΔH should be closer to those found in the cosolution of the two homopolymers or in the solution of the polymer A62 alone. In other words, as the blocks become more decoupled, T_t should drop and ΔH increase until they reach the values shown by the homopolymers alone. In our experiments, insertion of the linker had no significant effect on T_t and ΔH; therefore, the influence of the E-block on the A-block cannot be interpreted in terms of a dynamic and cooperative propagation along the polymer chain of a state of disorder from the E-block to the A-block through the direct link between them.

Comparison of the ITT in diblock and triblock elastin-like copolymers with different ratios between the A- and E-blocks

A new set of diblock copolymers provided further support for the hypothesis in this work. The diblock copolymers E50A20, E50A40, and E50A60 have the same length of the E-block but increasing lengths of the A-block. The DSC thermograms for solutions of the three diblocks at pH 2.5 and 7.0 can be seen in Fig. 2. For polymer E50A20, transitions for both the E-block and A-block are evident at pH values below the pK_a. In this particular case, the endotherm is clearly resolved into two peaks that can be assigned to the individual transitions of the two blocks. The two individual temperature peaks for E50A20 are closer to each other than in the cosolution, which shows that although there is a mutual influence between the two blocks, there is still some independency in their transitions. Additionally, the single temperature peak observed in copolymers E50A40 and E50A60 is midway between the two temperature peaks found in the cosolution. The integrated value of the combination of those two peaks ($\Delta H = 18.6\ J \cdot g^{-1}$) is again slightly higher than that expected for addition of the enthalpy of the two blocks with the mass ratio existing in the polymer E50A20 ($\Delta H = 15.1\ J \cdot g^{-1}$). Detailed values for T_t and ΔH can be found in Table 2. Only one peak is apparent for the other two diblock copolymers, but again the integrated area of that peak is significantly higher than the double contribution from the two blocks in the particular E-block/A-block mass ratio of each copolymer. If we consider the differences in hydrophobic hydration and the mutual influence, the more polar E-block will cause a decrease in the hydrophobic hydration in the A-block, whereas the more apolar A-block will cause an increase in the hydrophobic hydration in the E-block. As we have seen from the experimental results, the latter effect seems to be more pronounced.

TABLE 2 Transition temperatures for the polymers investigated

	pH 2.5			pH 7.0	
Polymer	$T_{tH}\|_E$ in °C	$T_{tH}\|_A$ in °C	ΔH /J · g^{-1}	$T_{tH}\|_A$ in °C	ΔH /J · g^{-1}
E50A20	31.6	34.2	18.6	*62.6	0
E50A40	- -	31.7	23.5	43.2	8.3
E50A60	- -	31.9	25.4	38.6	11.8
E50-G_L-A60	- -	32.0	24.1	38.8	11.3
E100A40	29.7	32.0	21.4	43.8	5.5
E50A20E50	28.5	- -	3.4	*75.3	0
E50A40E50	29.3	32.2	20.3	47.1	4.3
E50A60E50	30.7	32.0	21.9	41.7	6.3
E50A20E50A20	29.8	34.9	17.5	60.1	1.2

T_{tH}: Transition temperature in heating ($|_E$ of E-block. $|_A$ of A-block)
ΔH: Enthalpy of the whole transition of the different polymers.
*Data obtained after fitting to a sigmoidal function.

As the pH increases, the transition of the E-block shifts to higher temperatures and disappears when the pH exceeds the pK_a of the carboxyl group ($pK_a = 4.5$). Fig. 4 shows the dependence of the DSC endotherm as a function of pH for the diblock copolymer E50A60. Plots of T_t and ΔH versus pH can be seen in Fig. 5 for all diblock copolymers. Above that pH, the existing endotherm corresponds exclusively to the transition of the A-block. T_t and ΔH values for this isolated transition of the A-block in the three diblock copolymers are different, with T_t increasing as the length of the A-block decreases. At first glance, the relationship between the mean polarity of the three diblocks and the different T_t and ΔH values observed appears clear. Thus, the E-block, which has a constant length in the three diblock copolymers, is in a polyanionic state with high polarity, and therefore the mean polarity of these copolymers decreases as the A-block, which is predominantly hydrophobic, increases in length. In this sense, the diblock copolymer with the highest mean polarity (E50A20) shows the highest T_t and lowest ΔH, and that with lowest mean polarity (E50A60) shows the opposite trend. However, in contrast to what would be expected, this relationship is not linear as regards the length of the A-block, as can readily be seen in Fig. 6, where the T_t and ΔH values are plotted against the molar fraction of the A-block for these diblock copolymers. The dependence of T_t and ΔH on the A-block length is clearly not linear as the influence of the charged E-block is more intense for the E50A20 diblock, whereas it is less so as the A-block increases further in length. These results are therefore clear evidence that the mean

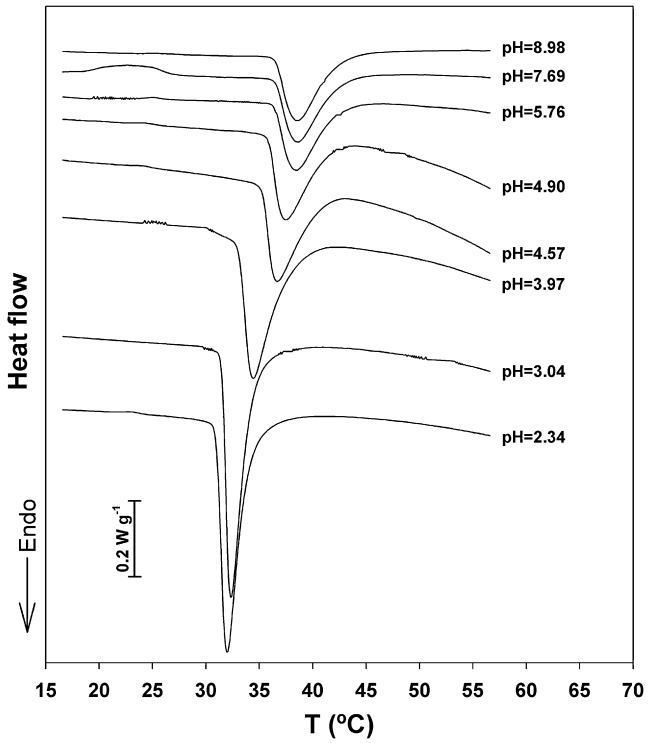

FIGURE 4 DSC thermograms in a heating run ($5°C \cdot min^{-1}$) for the diblock copolymer E50A60 ($50\ mg \cdot mL^{-1}$) at different pH values.

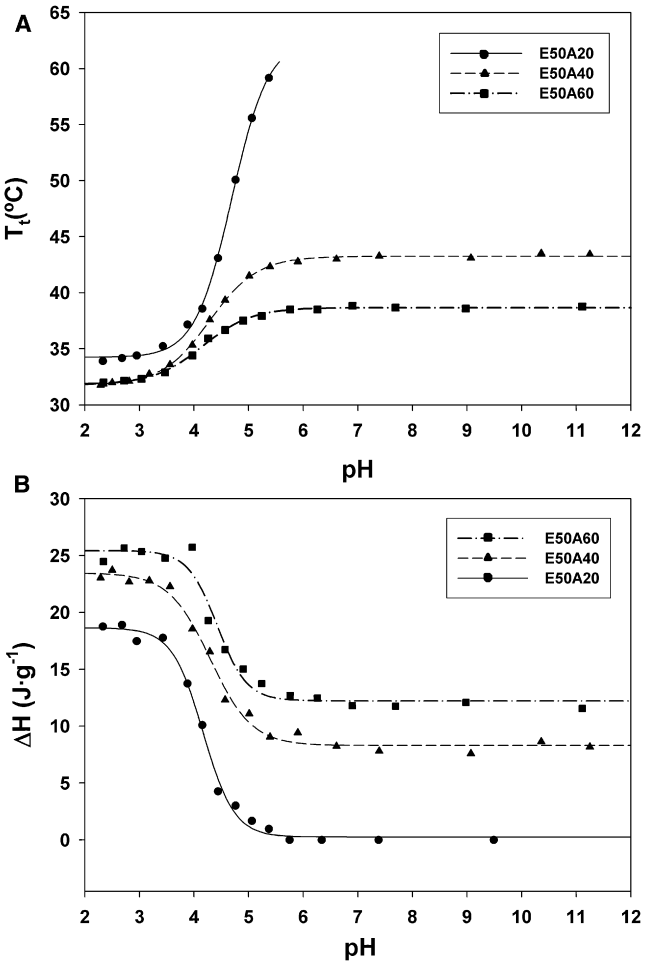

FIGURE 5 Plot of T_t (*A*) and ΔH (*B*) versus pH for the diblock copolymers E50A20, E50A40, and E50A60.

polarity alone cannot fully explain the differences in T_t and ΔH found in the ITT of these ELPs.

Further evidence in this direction can be found in the series of triblock ELPs E50AXE50 ($X = 20, 40, 60$). The DSC thermograms for these copolymers can be seen in Fig. 2 for two selected pH values (2.5 and 7.0), and precise values of T_t and ΔH can be found in Table 2. Below the pK_a, both transitions are again evident. In some cases, the two peaks are clearly distinguishable and, again, the enthalpy values are significantly higher than would be expected from the double contribution of the two blocks in all cases. Once more, a certain mutual influence between the two types of blocks can be deduced by the small shift in peak temperatures compared with the values found in the cosolutions. As is the case with the diblock copolymers, a clearer influence can be seen at pH values above pK_a. The dependence between T_t and ΔH, and the mean polarity of the chain (the polarity increases with $f_E = 1 - f_A$) are plotted in Fig. 6. Two facts are evident from an inspection of that plot. First, the lack of a linear trend in this series of triblock copolymers is again evident, and second, a comparison between the two series also provides additional support for our hypothesis regarding the role of the amino-acid sequence. This becomes clear when one compares E50A20 with E50A40E50. The A-block/E-block ratio is the same for these two copolymers, which implies a practically identical mean polarity at that pH (pH 7.0), although their T_t values are significantly different (up to 15.5°C). ΔH is also clearly different, going from 4.3 to $0.5\ J \cdot g^{-1}$. In addition, the dependence of T_t and ΔH on the mean polarity seems to be clearly different for the diblock and triblock copolymers, as deduced from the different trends shown by the respective curves plotted in Fig. 6. It is therefore clear that the amino-acid arrangement along the polymer chain plays a highly significant role in determining the parameters of the ITT.

These results must, however, be treated with some caution since the increase in the A-block length, while keeping the E-block constant, causes significant changes in the molecular masss. Although this intrinsic parameter is known to affect the T_t and ΔH values of ELPs, previous studies (19) have shown that this influence is only relevant for low molecular masss. Nevertheless, some effect—namely, a small increase in ΔH and a decrease in T_t as molecular mass increases—is still expected for these high-molecular-mass polymers. Although these small effects are unlikely to be the cause of the huge change observed for T_t, studies of additional polymers in which both molecular mass and mean polarity are constant, and only the arrangement of the amino acids along the chain changes, are required.

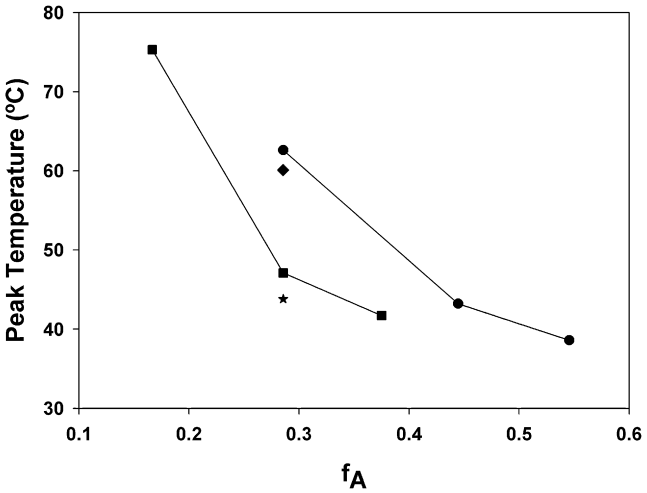

FIGURE 6 Plot of T_t versus molar fraction of the A-block, where f_A is the molar fraction of the A-block (in mols of pentapeptides) and f_E is the molar fraction of the E-block ($f_A + f_E = 1$), for the diblock copolymers E50A20, E50A40, and E50A60 (●); triblock copolymers E50A20E50, E50A40E50, and E50A60E50 (■); diblock copolymer E100A40 (★); and tetrablock copolymer E50A20E50A20 (◆) in aqueous solution at pH 7.0.

Exclusive influence of the block distribution and amino-acid sequence on the ITT

To definitively isolate the effect of the amino-acid sequence on the ITT, the behavior found in the block copolymer series E100A40, E50A40E50, and E50A20E50A20 was analyzed. These three copolymers show the same molar fraction of each block and even the same number and type of constituent amino acids, and therefore strictly the same mean polarity. In addition, all three have exactly the same molecular mass. The thermograms for those polymers at pH 2.5 and 7.0 can be seen in Fig. 2, and the T_t and ΔH values at these pHs can be found in Table 2. The quantitative dependence of T_t and ΔH on pH is plotted in Fig. 7.

The block copolymers in this set show the same molecular mass and mean polarity. Despite this, the huge behavioral differences between them are clear. In agreement with previous results, the T_t associated with the A-block is modified by the charged groups of the E-block, and this modification depends on the block sizes (lengths) in the di-, tri-, and tetrablock architectures. This variation of ITT with A-block size becomes more evident for pH values above the pK_a. Indeed, T_t increases enormously as the length of the A-blocks decreases, and the A-block is more fragmented and dispersed in the polymer chain. This increase is higher if this block is capped at both ends by a charged E-block (triblocks) or when it is split in two and surrounded by E-blocks (tetrablock). Curiously, the T_t and ΔH values for E100A40 are clearly different from the other two block copolymers in this set but are almost the same as those found for the diblock E50A40. In this sense, it is clear that the full length of the E-block is unable to affect the behavior of the A-block. Thus, from the data presented here, it appears that doubling

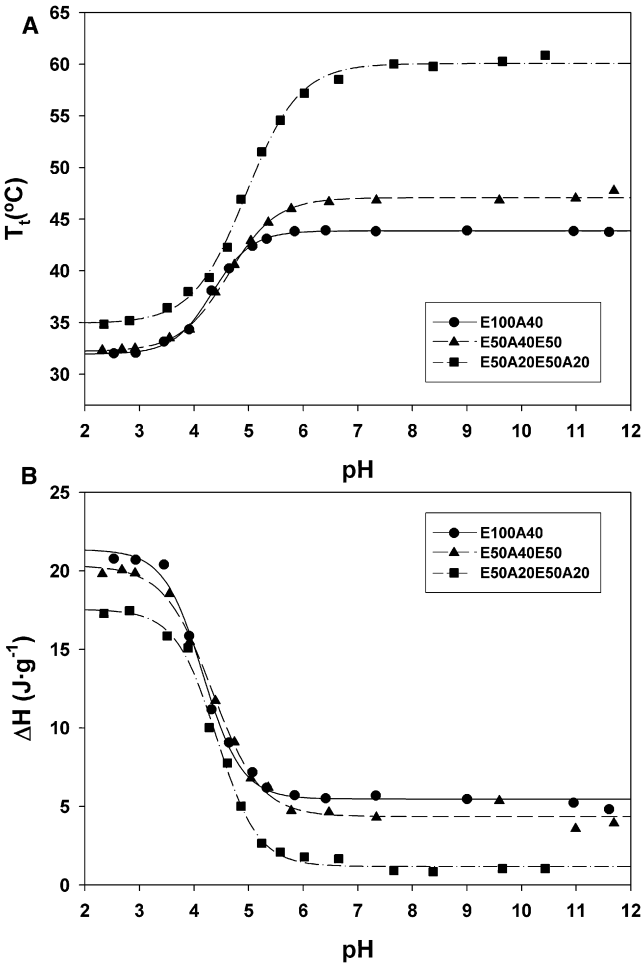

FIGURE 7 Dependence of T_t (*A*) and ΔH (*B*) on the pH for the diblock copolymer E100A40, triblock copolymer E50A40E50, and tetrablock copolymer E50A20E50A20.

the length of the E-block from E50 to E100 results in only a small, almost negligible shift in T_t.

CONCLUSIONS

We have seen in this work that the arrangement of block-copolymer architectures affects the behavior of the individual blocks, as both T_t and ΔH for the individual homopolymers change in the different block-copolymer molecular architectures investigated, thus showing a clear mutual influence between the different blocks. This fact has been reported previously but has always been attributed to a combination of changes in mean polarity and molecular mass. This influence is not caused by the transmission of the ordering state from one block to the other in a dynamical intrachain cooperative phenomenon, as was shown by the inclusion of a glycine linker between the two blocks. Additionally, these results show that T_t and ΔH depend not only on the polymer's mean polarity, but also, for a given composition, on the arrangement of amino acids along the polymer chain or,

equivalently, the distribution of polar and apolar regions along the polymeric chain. The prediction of T_t and ΔH by taking into account only the mean polarity and molecular mass is therefore only applicable to homopolymers of regular sequence. Indeed, T_t and ΔH for more complex polymers should be determined using models that reflect and quantify not only the mean polarity of the polymer chain, but also the distribution of different polar/apolar domains, and the chances and power they have for mutual influences.

We thank R. García for technical assistance in producing the polymers.

This work was supported by the Junta de Castilla y Leon (VA087A06, VA016B08, and VA030A08), the Ministerio de Ciencia e Innovación (MAT2007-66275-C02-01 and NAN2004-08538), and the Marie Curie Research Training Network Biopolysurf (MRTN-CN-2004-005516).

REFERENCES

1. Rodríguez-Cabello, J. C., J. Reguera, A. Girotti, F. J. Arias, and M. Alonso. 2006. Genetic engineering of protein-based polymers: the example of elastin-like polymers. *Adv. Polym. Sci.* 200:119–167.
2. Rodríguez-Cabello, J. C., J. Reguera, A. Girotti, M. Alonso, and A. M. Testera. 2005. Developing functionality in elastin-like polymers by increasing their molecular complexity: the power of the genetic engineering approach. *Prog. Polym. Sci.* 30:1119–1145.
3. Mcpherson, D. T., C. Morrow, D. S. Minehan, J. G. Wu, E. Hunter, et al. 1992. Production and purification of a recombinant elastomeric polypeptide, G-(VPGVG)19-VPGV, from *Escherichia coli*. *Biotechnol. Prog.* 8:347–352.
4. Kita-Tokarczyk, K., J. Grumelard, T. Haefele, and W. Meier. 2005. Block copolymer vesicles—using concepts from polymer chemistry to mimic biomembranes. *Polymer (Guildf.).* 46:3540–3563.
5. Urry, D. W. 1993. Molecular machines—how motion and other functions of living organisms can result from reversible chemical changes. *Angew. Chem. Int. Ed. Engl.* 32:819–841.
6. San Biagio, P. L., F. Madonia, T. L. Trapane, and D. W. Urry. 1988. The overlap of elastomeric polypeptide coils in solution required for single-phase initiation of elastogenesis. *Chem. Phys. Lett.* 145:571–574.
7. Urry, D. W., C. H. Luan, C. M. Harris, and T. Parker. 1997. Protein-based materials with a profound range of properties and applications: the elastin ΔTt hydrophobic paradigm. *In* Proteins and Modified Proteins As Polymeric Materials. K. McGrath and D. Kaplan, editors. Birkhäuser, Boston. 133–177.
8. Rodríguez-Cabello, J. C., M. Alonso, T. Perez, and M. M. Herguedas. 2000. Differential scanning calorimetry study of the hydrophobic hydration of the elastin-based polypentapeptide, poly(VPGVG), from deficiency to excess of water. *Biopolymers.* 54:282–288.
9. Tanford, C. 1973. The Hydrophobic Effect: Formation of Micelles and Biological Membranes. Wiley, New York.
10. Urry, D. W., T. L. Trapane, and K. U. Prasad. 1985. Phase-structure transitions of the elastin polypentapeptide-water system within the framework of composition-temperature studies. *Biopolymers.* 24:2345–2356.
11. Manno, M., A. Emanuele, V. Martorana, P. L. San Biagio, D. Bulone, et al. 2001. Interaction of processes on different length scales in a bioelastomer capable of performing energy conversion. *Biopolymers.* 59:51–64.
12. Rodríguez-Cabello, J. C., J. Reguera, M. Alonso, T. M. Parker, D. T. McPherson, et al. 2004. Endothermic and exothermic components of an inverse temperature transition for hydrophobic association by TMDSC. *Chem. Phys. Lett.* 388:127–131.
13. Li, B., D. O. V. Alonso, B. J. Bennion, and V. Daggett. 2001. Hydrophobic hydration is an important source of elasticity in elastin-based biopolymers. *J. Am. Chem. Soc.* 123:11991–11998.
14. Li, B., D. O. V. Alonso, and V. Daggett. 2001. The molecular basis for the inverse temperature transition of elastin. *J. Mol. Biol.* 305:581–592.
15. Gross, P. C., W. Possart, and M. Zeppezauer. 2003. An alternative structure model for the polypentapeptide in elastin. *Z. Naturforsch. [C].* 58:873–878.
16. Butler, J. A. V. 1937. The energy and entropy of hydration of organic compounds. *Trans. Faraday Soc.* 33:229–238.
17. Urry, D. W. 2004. The change in Gibbs free energy for hydrophobic association—derivation and evaluation by means of inverse temperature transitions. *Chem. Phys. Lett.* 399:177–183.
18. Urry, D. W. 2006. What Sustains Life? Consilient Mechanisms for Protein-Based Machines and Materials. Springer-Verlag, New York.
19. Girotti, A., J. Reguera, F. J. Arias, M. Alonso, A. M. Testera, et al. 2004. Influence of the molecular mass on the inverse temperature transition of a model genetically engineered elastin-like pH-responsive polymer. *Macromolecules.* 37:3396–3400.
20. Luan, C.-H., and D. W. Urry. 1999. Elastic, plastic, and hydrogel protein-based polymers. *In* Polymer Data Handbook. J. E. Mark, editor. Oxford University Press, New York. 78–89.
21. Reguera, J., J. M. Lagaron, M. Alonso, V. Reboto, B. Calvo, et al. 2003. Thermal behavior and kinetic analysis of the chain unfolding and refolding and of the concomitant nonpolar solvation and desolvation of two elastin-like polymers. *Macromolecules.* 36:8470–8476.
22. Meyer, D. E., and A. Chilkoti. 2002. Genetically encoded synthesis of protein-based polymers with precisely specified molecular mass and sequence by recursive directional ligation: examples from the elastin-like polypeptide system. *Biomacromolecules.* 3:357–367.
23. Dreher, M. R., D. Raucher, N. Balu, O. M. Colvin, S. M. Ludeman, et al. 2003. Evaluation of an elastin-like polypeptide-doxorubicin conjugate for cancer therapy. *J. Control. Release.* 91:31–43.
24. Chilkoti, A., M. R. Dreher, and D. E. Meyer. 2002. Design of thermally responsive, recombinant polypeptide carriers for targeted drug delivery. *Adv. Drug. Deliv. Rev.* 54:1093–1111.
25. Betre, H., W. Liu, M. R. Zalutsky, A. Chilkoti, V. B. Kraus, et al. 2006. A thermally responsive biopolymer for intra-articular drug delivery. *J. Control. Release.* 115:175–182.
26. Trabbic-Carlson, K., D. E. Meyer, L. Liu, R. Piervincenzi, N. Nath, et al. 2004. Effect of protein fusion on the transition temperature of an environmentally responsive elastin-like polypeptide: a role for surface hydrophobicity? *Protein Eng. Des. Sel.* 17:57–66.
27. Furgeson, D. Y., M. R. Dreher, and A. Chilkoti. 2006. Structural optimization of a ''smart'' doxorubicin-polypeptide conjugate for thermally targeted delivery to solid tumors. *J. Control. Release.* 110:362–369.
28. Sallach, R. E., M. Wei, N. Biswas, V. P. Conticello, S. Lecommandoux, et al. 2006. Micelle density regulated by a reversible switch of protein secondary structure. *J. Am. Chem. Soc.* 128:12014–12019.
29. Dreher, M. R., A. J. Simnick, K. Fischer, R. J. Smith, A. Patel, et al. 2008. Temperature triggered self-assembly of polypeptides into multivalent spherical micelles. *J. Am. Chem. Soc.* 130:687–694.
30. Wright, E. R., R. A. McMillan, A. Cooper, R. P. Apkarian, and V. P. Conticello. 2002. Thermoplastic elastomer hydrogels via self-assembly of an elastin-mimetic triblock polypeptide. *Adv. Funct. Mater.* 12:149–154.
31. Wu, X. Y., R. Sallach, C. A. Haller, J. A. Caves, K. Nagapudi, et al. 2005. Alterations in physical cross-linking modulate mechanical properties of two-phase protein polymer networks. *Biomacromolecules.* 6:3037–3044.
32. Wu, X., R. E. Sallach, J. M. Caves, V. P. Conticello, and E. L. Chaikof. 2008. Deformation responses of a physically cross-linked high molecular mass elastin-like protein polymer. *Biomacromolecules.* 9:1787–1794.
33. Sambrook, J., E. Fritsch, and T. Maniatis. 1992. Molecular Cloning: A Laboratory Manual. CSHL Press, New York.
34. Girotti, A., J. Reguera, J. C. Rodríguez-Cabello, F. J. Arias, M. Alonso, et al. 2004. Design and bioproduction of a recombinant multi(bio)functional elastin-like protein polymer containing cell adhesion sequences for tissue engineering purposes. *J. Mater. Sci. Mater. Med.* 15:479–484.